

Veritas: Answering Causal Queries from Video Streaming Traces

Chandan Bothra^{*1}, Jianfei Gao^{*1}, Sanjay Rao¹, and Bruno Ribeiro¹

¹Purdue University

April 20, 2022

Abstract

In this paper, we seek to answer *what-if* questions – i.e., given recorded data of an existing deployed networked system, what would be the performance impact if we changed the design of the system (a task also known as causal inference). We make three contributions. First, we expose the complexity of causal inference in the context of adaptive bit rate video streaming, a challenging domain where the network conditions during the session act as a sequence of latent and confounding variables, and a change at any point in the session has a cascading impact on the rest of the session. Second, we present Veritas, a novel framework that tackles causal reasoning for video streaming without resorting to randomized trials. Integral to Veritas is an easy to interpret domain-specific ML model (an embedded Hidden Markov Model) that relates the latent stochastic process (intrinsic bandwidth that the video session can achieve) to actual observations (download times) while exploiting control variables such as the TCP state (e.g., congestion window) observed at the start of the download of video chunks. We show through experiments on an emulation testbed that Veritas can answer both counterfactual queries (e.g., the performance of a completed video session had it used a different buffer size) and interventional queries (e.g., estimating the download time for every possible video quality choice for the next chunk in a session in progress). In doing so, Veritas achieves accuracy close to an ideal oracle, while significantly outperforming both a commonly used baseline approach, and Fugu (an off-the-shelf neural network) neither of which account for causal effects.

1 Introduction

A central theme of data-driven networking is answering *what-if* questions — given data obtained from a real-world deployment of an existing system, we want to infer what would have happened if we had used a different system design. For instance, given data collected from real video streaming sessions, a video publisher may wish to understand the performance if a different Adaptive Bitrate (ABR) algorithm were used (Figure 1), or if a new video quality (e.g., an 8K resolution) were added to the ABR selection, or an existing bit rate

choice were removed (e.g., during the COVID crisis, many video publishers restricted the maximum bit rate [3]). Answering *what-if* questions of this nature is also known as *causal reasoning*. Causal inference considers the effect of events that did not occur while the data was being recorded [33], and has been explored in domains as diverse as economics [8] and epidemiology [35].

Shortcomings of traditional (associational) machine learning. Several widely used machine learning (ML) tools are inadequate for causal inference. Many approaches (e.g., neural networks and decision trees) merely capture correlations in collected data, limiting them to *associations predictions*, i.e., predictions that are related to associations between observations in a deployed system. Associations, however, are inadequate to answer causal questions. For instance, people carrying umbrellas on a sunny morning is a good predictor of rain in the afternoon. However, forbidding people to carry umbrellas in the morning does not *prevent* rain in the afternoon. Similarly, in video streaming, an ABR algorithm could choose lower bitrates when network conditions are poor, resulting in an association between lower video bitrates and rebuffering events. However, decreasing bitrate will not *cause* more rebuffering events – rather, the opposite is likely to happen. Other approaches such as Reinforcement Learning and Randomized Control Trials allow reasoning about a redesigned system but require *active interventions* that involve changing a system, and observing its performance among real users. These approaches could be disruptive to the performance of real users, and cannot answer *what-if* questions about past sessions (§2).

Confounders in video streaming. In contrast to the above approaches, our work focuses on *causal inference* on *passively collected data*, which is not disruptive to the performance of live users. We consider causal inference not only about how the proposed change would affect sessions in the future (also referred to as *interventional inference*) but also how it would have affected a given session in the past (also referred to as *counterfactual inference*). We expand on the distinctions in §2.1.

While causal inference can benefit many networking tasks, in this work we focus on video streaming. First, it is a domain

^{*}These authors contributed equally to this work.

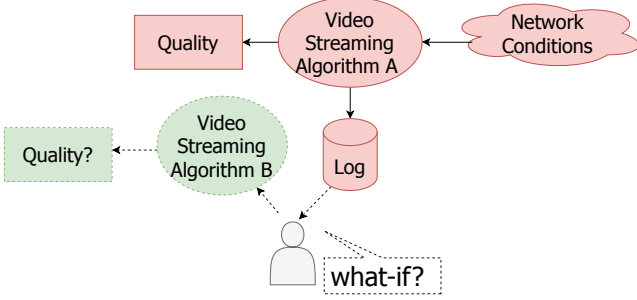


Figure 1: Example *what-if* question asked by a network designer: what would be the quality if algorithm B had been used instead of A under the same network conditions?

where there has been much interest in using data to drive design optimizations [10, 22, 24, 28, 40, 47]. Second, video streaming relies on adaptive bit rate (ABR) algorithms, where decisions made by the algorithm depend on network conditions, which in turn impact observable measurements. Owing to the adaptive nature, the *network conditions encountered during the session* act as a *sequence of latent confounding variables*, resulting in complex spurious correlations in data, which can impair the use of common ML approaches. We demonstrate this by showing that Fugu [47], a recent work that uses a neural network to predict download times in video sessions, can suffer significant biases when asking causal questions (§2.2).

Cascading effects complicate causal inference in video streaming. The dynamic nature of video streaming makes causal inference a challenging task. Consider asking the following *what-if* question for a recorded video session: what if bitrate b' rather than the original b had been chosen for video chunk $n \geq 1$, $b' \neq b$? This *what-if* change (from b to b' at chunk n) has a cascading impact on the session’s future buffer occupancy, and bitrate selection decisions, as well as the start times of future chunk downloads. Thus, all observed variables describing chunk $n' \geq n$ can potentially change due to a different decision for chunk n . Here, the data recorded in the session after chunk n no longer represents what will happen in the session even if no other changes were made in the future.

Taming the complexity of causal inference with Veritas. Motivated by the above challenges we design **Veritas**, a novel framework for answering causal queries for video streaming. Rather than complex ML models, or resort to randomized trials, Veritas only relies on easy-to-interpret and low-complexity ML models, while only requiring pre-recorded data. The challenge that Veritas tackles is *abduction* [33, Section 4.2.4], which involves (i) inferring a set of likely values for latent variables consistent with the observations; and (ii) modeling the proposed changes to return the answer to a *what-if* query using the inferred latent variables. While abduction is challenging in general, the key insights of Veritas are (a) a careful selection of control variables (the TCP states at the

start of each chunk download) that simplifies the causal task, and (b) a ML method to perform abduction that is principled, yet accessible and easy to interpret given it leverages domain insights.

More specifically, as part of Veritas, we have designed a domain-specific ML model that relates the latent stochastic process (intrinsic bandwidth that the video session can achieve if TCP were in steady state throughout the session) to actual observations (actual throughput observed by chunk downloads), when also given a sequence of additional control variables in the form of the TCP states at the start of each chunk download. This control is needed since the actual observed throughput depends on the TCP state of the connection (e.g., whether slow-start is in progress), and the size of the downloaded object. The control allows us to “invert” the observed throughput variables in order to get the latent bandwidth variables.

To ensure we represent the statistical dependencies in the latent bandwidth time series during the inversion process, we develop an Embedded Hidden Markov Model (EHMM), which embeds a domain-specific model for the emission process. A Bayesian posterior sampling of the EHMM allows us to capture the uncertainty inherent in the combination of our inversion, stochastic modeling, and the data. Once a sampled inverted bandwidth process is obtained, we can now directly evaluate the proposed changes, and return the answer to the *what-if* query. Rather than a single *point estimate*, Veritas provides a range of potential outcomes reflecting the inherent uncertainty in inferences that can be made from the data.

Evaluation. We evaluate Veritas with respect to its ability to answer a range of *what-if* causal queries including the impact of (i) changing the ABR algorithm; (ii) changing the buffer size; and (iii) changing the set of video qualities that the ABR algorithm could select from using an emulation testbed. Our evaluation approach involves emulating a video streaming system in its original setting, mimicking a deployed system with bandwidth traces that serve as the ground truth. We then apply Veritas on the logs of the deployed systems (excluding the ground truth bandwidth traces) and use Veritas’s abduction to predict the impact of the *what-if* change. We compare the predictions from Veritas with predictions from a baseline approach that uses the logs directly without explicit causal adjustments, and an oracle approach that knows the exact ground truth bandwidth values. Across the board, Veritas returns significantly more accurate results to causal inferences than the baseline approach, and close to the ground truth values. For example, when changing to high video qualities, Veritas predicted negligible rebuffering ratio across all the traces, close to the oracle, while Baseline predicted a much higher median rebuffering ratio value of around 6.7%.

We also evaluate Veritas’s ability to answer interventional queries (inferences related to the future) by focusing on its ability to predict the download time of future video chunks given information about past chunk download statistics. Note

that Veritas must be able to make predictions under new unseen scenarios (e.g., session logs of the previously deployed ABR algorithm may only contain certain chunk size sequences, while the intervention may need to make decisions about more general sequences). We show that for such interventional queries, Veritas achieves much higher accuracies than Fugu [47], which relies on an associational method. Overall, the results show the importance and benefits of Veritas.

2 Background and Motivation

In this section, we motivate the need for causal reasoning, and why ML tools used for associational predictions, and approaches such as Reinforcement Learning and Randomized Control Trials fall short. We illustrate this in the context of video streaming, and show how a state-of-the-art video streaming system [47] that uses associational reasoning for a causal task falls short.

2.1 Causal vs. Associational Queries

Video streaming today typically involves splitting video into chunks, each encoded at multiple qualities. Clients pick qualities for each chunk using Adaptive Bit Rate (ABR) algorithms so as to balance between achieving high video quality, while avoiding rebuffering based on network conditions [6, 17, 19, 26, 38, 44, 48].

Consider data collected from a video streaming system, where for each session information is collected regarding the chunk size and the download time. Two questions may be of interest to a designer:

Q1. Given a set of observations of chunk sizes and download times of a video session, if the video session were going to next download a chunk of size s , what would be the download time?

Q2. Given a set of observations of chunk sizes and download times of a video session, if the designer had *intervened* in the session and had asked to next download a chunk of size s' , $s' \neq s$, what would be the download time?

Question **Q1** pertains to passively observing the system at hand with its existing ABR algorithm and settings. These offline observations can be used to make predictions about the system under similar conditions. More broadly, an *associational prediction* seeks to predict outcomes of a system without interfering (*intervening*) with its operation. In contrast, many real-world networking tasks are like **Q2**, which require going beyond passively predicting the outcomes of an existing system. These tasks require *causal inference*, which predicts the outcome of an intervention, a change in the way the system operates. Specifically, **Q2** pertains to the impact of an *interventional change* to the system design: specifically using a different decision procedure that leads to a chunk of size s' being downloaded rather than the original ABR's decision of downloading size s . More generally, the designer may wish to understand the implications on performance if

some aspect of the system were changed (e.g., changing the set of video qualities the client could choose from, the buffer size, or the ABR algorithm).

We next define the two types of causal inference algorithms of interest in our work, refining a common definition of *learning algorithms* [27, Chapter 1.1].

Definition 1 (Learning interventional inference for network tasks). *Given (i) a networking task over an unseen session with a new method; (ii) training experience (e.g., existing recorded sessions) obtained with an old method; and (iii) a performance measure; then, a computer program is said to learn interventions if its prediction performance in the new method at the task (new sessions) improves if given more experience (e.g., given more recorded sessions with the old method).*

We further refine Definition 1 for counterfactuals.

Definition 2 (Learning counterfactual inference for network tasks). *Given (i) training experience (e.g., existing recorded sessions) running an old method; (ii) a new method; and (iii) a performance measure, a computer program is said to learn to perform counterfactual inference if its ability to predict the performance of the new method if it had been used in place of the old method in the same recorded sessions improves if given more experience (e.g., given more recorded sessions with the old method).*

In this work we introduce Veritas, a computer program that is able to perform both interventional and counterfactual learning (Definitions 1 and 2, respectively).

2.2 Challenges with causal queries

Associational approaches are inadequate. Most ML methods work by learning associations in existing data, and, hence, are only appropriate for associational predictions. Unfortunately, the result of an associational prediction may be wildly inaccurate for a causal question. We next illustrate this in the context of Fugu [47], which uses an associational ML model for a causal query. Specifically, Fugu [47] proposes a neural network which predicts the download time of a video chunk given its size, and given the size and the download times of the previous K chunks. Consider Fugu trained with data obtained from the deployment of an ABR algorithm, say Algorithm A. This effectively trains Fugu to answer the associational Question **Q1** which involves predicting the download time for the chunk size selected by Algorithm A (§2.1). However, consider that the trained Fugu model is actually deployed as a predictor in a real video streaming session, in a manner that *intervenes* with bit rate selection. That is, at any given time step of a live session, Fugu is used to predict the download times for *all possible chunk sizes*, and an appropriate chunk size is selected based on these predictions. Then, effectively, Fugu is being used to tackle the causal query **Q2** (§2.1).

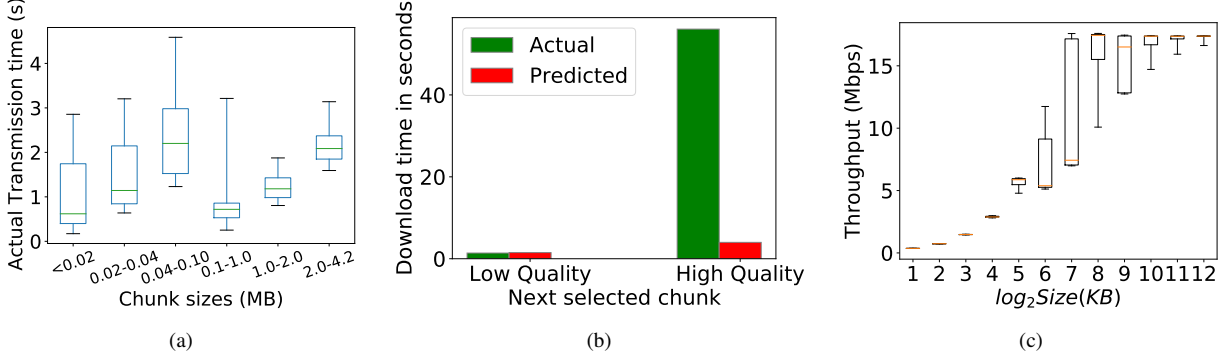


Figure 2: (a) Distribution of download times for different groups of chunk sizes with the MPC algorithm on a subset of FCC traces [1]. The relationship is not monotonic owing to the adaptive nature of the algorithm. (b) Prediction error in Fugu [47] with causal queries. (c) Variance in observed throughput with chunk size for same emulated network bandwidth.

Unfortunately, the associational approach suffers from a bias because the deployed ABR algorithm A tends to pick lower (resp. higher) sized chunks when network bandwidth is bad (resp. good). Consequently, the download time with an ABR algorithm many not necessarily show the expected dependence with size. To illustrate this, we conducted controlled experiments where we trained Fugu on 100 traces, 50 with poor network conditions [0-0.3 Mbps] and 50 with good network condition [9-10 Mbps] with the MPC algorithm in an emulation testbed (details in §4) using the FCC throughput traces [1]. Figure 2(a) presents the download time of all chunks across all the video sessions, with each boxplot corresponding to chunks with a particular size range. The figure shows that the download times do not grow in a linear fashion with chunk size, rather show a non-monotonic dependence. This is because of the adaptive bit rate selection described above.

We next test Fugu on a new trace with poor network conditions. We consider a point in time where the ABR algorithm has picked a sequence of lower quality chunks. We then use Fugu to answer the *what-if* questions, what would the download time be if (i) the next chunk selected were high quality; and (ii) the next chunk selected were low quality. Figure 2(b) shows the download times predicted by Fugu and the actual download times in each case. The figure shows that Fugu significantly underestimates download times for the high quality chunk, but does a good job for the low quality chunk. This is because Fugu uses an associational model that is effective at predicting download times for a chunk size that the deployed algorithm would have selected next, but not the download times if the chunk size had been forced to be a particular value. Consequently, while the model effectively predicts the download time of chunk sizes actually chosen by the deployed ABR, it performs poorly when answering the causal query *what would happen if an alternate size were chosen*.

Latent variables complicate causal queries. A potential alternative to the above approach is to consider the observed throughput when downloading a video chunk, defined as S/D .

where S is the size, and D the download time. For instance, the neural network from [47] could use a sequence of observed chunk throughputs, and predict the throughput of the next chunk. Unfortunately, the observed throughput itself is dependent on the size of chunks owing to TCP slow start effects [10, 28, 47]. Figure 2(c) presents a distribution of throughput for chunks in a given size range in controlled experiments using TCP where we emulated a constant network bandwidth of 18 Mbps in a client server setup, and sent payloads of varying sizes (2KB to 4MB). Note that the gap between payloads impacts whether TCP enters a slow-start restart phase [12]. The graph shows that for small sizes (less than the bandwidth delay product of the network), throughput is much smaller, while it is closer to the intrinsic network bandwidth for larger sizes. Note that for intermediate sizes (around 2^6 to 2^{10} Kilobytes) there is significant variability in throughput based on the gap between the transmission of two consecutive payloads, and whether TCP enters slow start restart or not. Thus, simply considering throughput is insufficient, and while it would be desirable to consider the intrinsic network bandwidth, this is a hidden variable not available in data.

2.3 Why not actively intervene?

Rather than making predictions by passively observing a system, some approaches can evaluate the impact of a design change by actively intervening (changing) the system, and observing the performance. These techniques include Randomized Control Trials (RCTs), A/B Testing, and Reinforcement Learning [41].

RCTs [15] can measure the effects of interventions. However, there are several disadvantages to RCTs. First, such trials may lead to degraded performance to some viewers. For instance, in the context of video streaming algorithm, even if chunk bitrates are chosen randomly without regard to network conditions, a chunk’s start time is not random as it still depends on the download end time of the previous chunk [39]. Another approach is to use **A/B testing** of a new

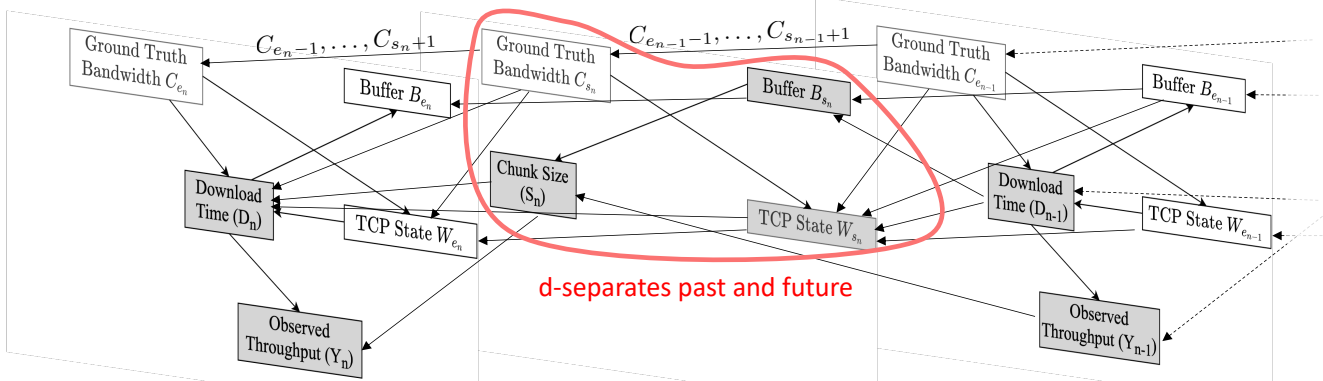


Figure 3: Causal model of (embedded) dependencies in an ABR algorithm starting at e_{n-1} , the arrival time of the $(n-1)$ -st chunk, until e_n , the arrival time of the n -th chunk. Shaded gray variables are observed, while white (unshaded) variables are hidden. A sufficient condition for a set U of variables to d -separate a set A and B is that all undirected paths in the DAG between A and B include at least one variable from U , and no such paths have arrows collide “head-to-head” in the variables in U .

design change. Since A/B testing can impact the performance of live users, it is only used in a conservative fashion if an offline analysis approach indicates the design change has sufficient potential. Thus, there remains a need to answer a question offline with trace data alone.

Reinforcement learning may be viewed as a sequential RCT in that the agent dynamically learns the best decisions to take at each state of the system. The collection of all pairs (best decisions, current system states) is denoted a *policy*. A drawback of RCTs in general, and reinforcement learning in particular, is that it only answers the question of which decisions, out of a set of tested decisions, are the best to take for a given system state. If our set of possible decisions changes, the RCT/RL tests must be run again on new sessions.

Another important point is that both RCTs and reinforcement learning cannot directly answer counterfactual queries, although their randomized (exploration) measurements may still be used by counterfactual estimators in some special cases (e.g., [9]). Hence, interventional methods may not be useful in some scenarios because they can only be tested in future sessions: Imagine seeing rare network conditions where a deployed algorithm performed poorly. Since these conditions are rare, we would like to know if a certain change to the algorithm would have significantly improved the performance. This is a counterfactual query and RCTs and reinforcement learning are generally not applicable in this scenario since the event is in the past, and any RCT to test a new intervention on the system can only be applied in future sessions.

3 Veritas: A causal inference framework for video streaming

In this section, we present Veritas, our framework for answering causal queries related to video streaming. We start by presenting a causal graph (DAG) which models the variables involved with video streaming, and the dependencies or causal relationships between them (§3.1). We then discuss how the DAG leads us to decide what adjustments are needed to iden-

tify a causal effect, and how to make the adjustment (§3.2). Finally, §3.3 discusses how Veritas puts all these methods together to perform counterfactual and interventional inference.

3.1 Modeling causal dependencies

A key factor that impacts the decisions made by a video streaming algorithm is the **Ground Truth Bandwidth (henceforth abbreviated as GTBW)**, which captures the bandwidth the network is intrinsically capable of, without considering dependence on size, and the slow start effects of the transport protocol – i.e., what the transport protocol would intrinsically see if it were running in steady state. We model the evolution of GTBW as a discrete process over discrete time intervals $t \in \{1, \dots, T\}$ (each of wall-clock time length of δ), with the GTBW during any time interval being a constant. Time is assumed to be discrete to simplify our approach, since δ can be as fine-grained as necessary.

Consider that the session downloads a series of chunks $1 \dots N$. Chunk $n \in \{1, \dots, N\}$ starts its download at time $s_n \in \{1, \dots, T\}$ and finishes at time $e_n \in \{s_n, \dots, T\}$. The variables that evolve over time are: (i) $C_t \in \mathcal{C}$, the average GTBW at time interval $((t-1)\delta, t\delta]$; (ii) B_t , the amount of buffer in the video player at time $t \in \{1, \dots, T\}$, and (iii) W_t , the TCP state at time t . The TCP state includes parameters such as the congestion window, slow start threshold, RTT, min RTT, time since last data send, and RTO.

The variables that evolve at each chunk request are: (i) the size (S_n) of the n -th requested chunk and (ii) D_n , its download time, $n = 1, \dots, N$. The throughput observed during the download (Y_n) can be calculated using the chunk size and download time.

Henceforth, for any random variable X we define the sequences $X_{a:b} := (X_a, \dots, X_b)$ and $X_{s_{a:b}} := (X_{s_a}, \dots, X_{s_b})$. Moreover, let $\mathcal{S} = \cup_{n=1}^N \{s_n\}$ and $\mathcal{E} = \cup_{n=1}^N \{e_n\}$ be the set of random variables of showing the discrete times where a chunk starts and ends downloading, respectively. We assume that the variables in $W_{s_{1:N}}, B_{s_{1:N}}, S_{1:N}, \mathcal{S}, \mathcal{E}$ and $Y_{1:N}$ (shown in shaded

gray in Figure 3) are generally *observed* variables in video streaming sessions (that is, all the information regarding them is either directly available, or can be calculated from the data). Note that TCP state information is easy to collect (e.g., using the *tcp_info* structure in Linux systems [5]). Further, although we could collect the information, we do not require the values $\{W_t\}_{t \in \{1, \dots, T\} \setminus \mathcal{S}}$, $\{B_t\}_{t \in \{1, \dots, T\} \setminus \mathcal{S}}$, and treat these variables as hidden.

Figure 3 shows a directed acyclic graph (DAG) describing the causal dependencies for video streaming. Note that Figure 3 only illustrates the embedded process of $\{C_t\}_{t \in \mathcal{S} \cup \mathcal{E}}$, $\{W_t\}_{t \in \mathcal{S} \cup \mathcal{E}}$, and $\{B_t\}_{t \in \mathcal{S} \cup \mathcal{E}}$, at the event times where a new chunk is requested or finishes downloading. It is important to note that the variables $C_{1:T}$, $W_{1:T}$, $B_{1:T}$ also evolve in the time between these chunk events, but for any time $t \in \{1, \dots, T\} \setminus \{\mathcal{S} \cup \mathcal{E}\}$ that happens between chunk start and end times, the random variables B_t depends only on B_{t-1} (just the video being played) and C_t depends only on C_{t-1} , but W_t depends on both W_{t-1} and C_{t-1} if there is an active chunk download at time t (and only on W_{t-1} if there is no active download).

The n -th chunk size S_n is influenced (through the ABR algorithm) by both the buffer state B_{s_n} at the start of download of chunk n and the last observed throughput Y_{n-1} (and possibly Y_{n-2}, \dots, Y_1 (not shown in the DAG)). The chunk size value S_n influences the download time D_n . Further, the TCP state W_{s_n} determines whether the TCP connection of the chunk download experiences slow start restart, initial congestion window etc., all of which together with S_n and C_{s_n}, \dots, C_{e_n} also influence the download time D_n . A key parameter of the TCP state is the gap since the last packet was transmitted. This in turn depends on the video application. When the buffer is full, the player does not send further requests, but when not full, it may trigger requests immediately. Hence, W_{s_n} itself depends on $B_{e_{n-1}}$, which defines a new chunk request at time s_n . Finally, as discussed above S_n and D_n together determine Y_n .

Confounders: The DAG in Figure 3 shows that $C_{1:T}$ are confounder variables between $S_{1:N}$, $D_{1:N}$, and $W_{s_{1:N}}$. Confounders are hidden variables (not available in the data) that jointly influence multiple observed variables. Moreover, we make the simplifying assumption that $C_{1:T}$ are not influenced by any other variable in the model (that is, chunk downloads do not impact the GTBW). Our model also assumes we are running a particular version of TCP (e.g., Cubic, or BBR) and cannot directly be used to model the impact of *what-if* questions where the TCP version itself might change. This would require modeling more intrinsic hidden factors such as the number of simultaneous flows in routers, etc..

3.2 Veritas abduction for causal queries

Since no other variables affect the confounder variables $C_{1:T}$ but $C_{1:T}$ directly or indirectly affect all other variables (i.e., all other variables are descendants of some variable in $C_{1:T}$),

if we could infer $C_{1:T}$ we would be able to handle any counterfactual or interventional query needed. This procedure to infer a confounder ($C_{1:T}$) to respond to causal queries is known as *abduction* [33, Section 4.2.4]. Abduction involves (i) “inverting” the observed variables to get the hidden confounders; and (ii) then modeling the proposed changes (assuming the hidden confounder values are now known) to return the answer to the *what-if* query. Abduction approaches in the ML literature typically rely on composable statistical models using high-level programming languages [11, 13, 29] that, unfortunately, do not effectively deal with the use of *if* statements and other deterministic decision functions common in networking. Hence, our work proposes the Veritas custom abduction method tailored to our task, described in the next few paragraphs.

The Veritas abduction of $C_{1:T}$. In our setting, abduction requires sampling the network GTBW given all the observations in a session:

$$C_{1:T} \sim P(c_{1:N} | S_{1:N}, D_{1:N}, B_{s_{1:N}}, W_{s_{1:N}}), \quad (1)$$

where $R \sim g$ denotes that random variable R is sampled with distribution g . Once the confounding variables $C_{1:T}$ are sampled given the observed variables, we can simulate the effect of the causal query in the sampled $C_{1:T}$ (now assumed known). The sampling in Equation (1) accounts for the non-unique nature of the “inversion”, imposing a distribution over the *what-if* query results. Obtaining $C_{1:T}$ requires connecting it to the observed variables, including the observed throughput $Y_{1:N}$, TCP states $W_{s_{1:N}}$, a sequence of buffer states $B_{s_{1:N}}$, and chunk sizes $S_{1:N}$. We discuss how Veritas achieves this next.

Abduction of $C_{1:T}$ via EHMMs. Veritas uses a special type of Hidden Markov Model (HMM) [45]. An HMM is specified by (i) a set of hidden states \mathcal{C} ; (ii) a matrix that captures the transition probabilities from one hidden state to another; (iii) a set of observations; (iv) a set of probabilities (a.k.a. emission probabilities), which capture the likelihood of a particular observation being generated from a given hidden state; and (v) an initial probability distribution over states. In our context, the GTBW sequence $C_{1:T} \in \mathcal{C}^T$ corresponds to the hidden states, while the throughput Y_n is the observation *jointly emitted* by the states $C_{s_n:e_n}$.

The importance of observing TCP states $W_{s_{1:N}}$. Note that in an HMM, because of the Markov property, given the hidden variable (C_{s_n}), the emissions (Y_n) are independent of the past emissions (Y_{n-1}, \dots, Y_1). In graphical model language we say C_{s_n} needs to d-separate Y_n and $\{Y_{n-1}, \dots, Y_1\}$. A sufficient condition for a set U of variables to d-separate a set A and B is that all undirected paths in the DAG between A and B include at least one variable from U , and no such paths have arrows collide “head-to-head” in the variables in U [33, Definition 1.2.3]. The challenge is that C_{s_n} *does not* d-separate Y_n and Y_{n-1}, \dots, Y_1 in the DAG of Figure 3.

In order to achieve this d-separation independence, Veritas conditions the entire HMM on the sequence of TCP

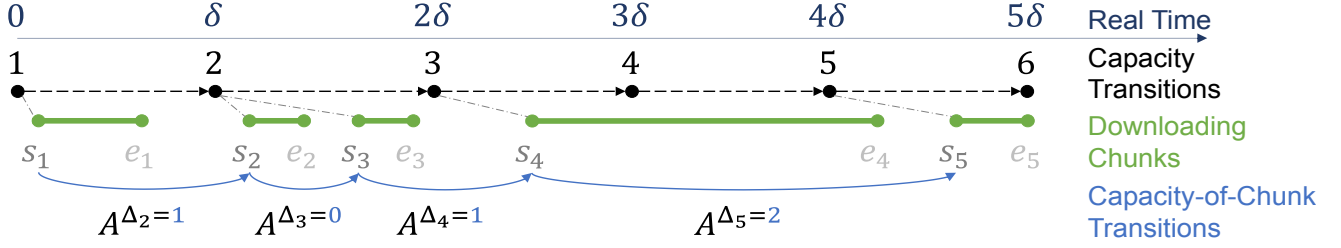


Figure 4: **Translation from Real Time Capacity Transition to Downloading Chunk Capacity Transition.** On the top, the GTBW evolves every δ time units. We assume C_t is constant in the interval $[(t-1)\delta, t\delta)$. In the middle lines shows five downloading chunks, beginning at s_n and ending at e_n , $n = 1, \dots, 5$. At the bottom, under the arrows, we show the number of GTBW transitions Δ_n between consecutive chunks. For example, chunk 2 and chunk 3 start at the same time window, so $\Delta_3 = 0$, while chunk 4 and chunk 5 both start at window 3 and 5 respectively, so $\Delta_5 = 2$.

and buffer¹ states at the chunk start times ($W_{s_{1:N}}$ and $B_{s_{1:N}}$), together with the sequence of requested chunk sizes ($S_{1:N}$). This conditioning ultimately allows us to *d-separate* Y_n and $\{Y_{n-1}, \dots, Y_1\}$ in the DAG of Figure 3. It is easy to check that the variables $C_{s_n}, W_{s_n}, B_{s_n}, S_n$ —circled in red in Figure 3—block any undirected paths between Y_n and $\{Y_{n-1}, \dots, Y_1\}$ in the DAG.

The Veritas embedded Markov chain. The HMM that Veritas uses (which we refer to as EHMM) also departs from standard HMM models in other ways. First, HMMs traditionally use common parameterized probability distributions (e.g., multinomial, Gaussian) to model emission probabilities. Instead, Veritas embeds a domain-specific model for its emissions. The model captures how GTBW, chunk sizes, and TCP states gets translated into observed throughput. Second, in traditional HMMs, each hidden state is associated with a single observation. However, in our context, observations are only associated with those hidden GTBW states where chunks are being downloaded. The hidden GTBW itself changes during the off periods where no chunks are being downloaded, and there are no observations available during this time. Further, it is possible that there are multiple chunks downloaded in the same time interval $((t-1)\delta, t\delta]$, $t \in \{1, \dots, T\}$. To handle this, Veritas’s EHMM allows each GTBW state to be associated with zero, one or more observations (corresponding to the number of chunks downloaded in the corresponding interval). Note that Veritas’s use of EHMM is consistent with prior work [6, 40], which has modeled TCP throughput evolution as a Markov process, but Veritas addresses complexities associated with embedding a custom emission process, *d-separation*, and the focus is on abduction for causal inference.

Hidden state transitions. As discussed in §3.1, evolution of GTBW is modeled as a discrete sequence $C_{1:T}$, where C_t denotes the average GTBW during time interval $((t-1)\delta, t\delta]$. Further, for simplicity, Veritas uses a quantized set of capacities to ensure the number of states is discrete. GTBW values C are quantized via a hyperparameter $\varepsilon > 0$. For instance, $\varepsilon = 0.5$ implies that the hidden states are $C =$

$\{0.0\text{Mbps}, 0.5\text{Mbps}, 1.0\text{Mbps}, \dots\}$. Both hyperparameters δ and ε may be kept as small as needed.

The sequence $C_{1:T}$ is modeled as a first-order Markov chain $P(C_t | C_1, \dots, C_{t-1}) = P(C_t | C_{t-1})$, $1 < t \leq T$. The conditional distribution $P(C_t | C_{t-1})$ is parameterized by a transition matrix A such that

$$A_{i,j} = P(C_t = j\varepsilon | C_{t-1} = i\varepsilon), \quad 1 < t \leq T. \quad (2)$$

For $t = 1$, since there are no transitions, we will directly model the initial distribution of GTBW by a distribution u , with hyperparameter $u_i = P(C_1 = i\varepsilon)$. Finally, given two hyperparameters, GTBW transition interval size δ and minimum GTBW discrepancy ε , we can model the GTBW evolution by the transition matrix A (Equation (2)) and the initial distribution u , thus can measure GTBW evolution distribution by $P(C_{1:T}) = P(C_1) \prod_{t'=2}^T P(C_{t'} | C_{t'-1})$.

Domain-specific model for emission process. As discussed in Section 3.1, for any chunk $1 \leq n \leq N$, with start time s_n and end time e_n , we will observe corresponding throughput Y_n , TCP state W_{s_n} and chunk size S_n . The throughput Y_n observed by video chunk n is a function of GTBW $C_{s_n:e_n}$, the starting TCP state W_{s_n} , and the chunk size S_n , and we want to test if an arbitrary GTBW can fit the observed chunk.

We develop a simple model of TCP to estimate Y_n , denoted by f (Algorithm 4 in the Appendix), which models congestion control with slow start, congestion avoidance and slow start restart (TCP SSR) [12]. If the network is idle and $W_{s_n}^{\text{last_send}}$ is greater than the retransmission time out $W_{s_n}^{\text{rto}}$, TCP SSR is triggered and the congestion window $W_{s_n}^{\text{cwnd}}$ and slow start threshold $W_{s_n}^{\text{ssthresh}}$ are updated according to the Linux kernel implementation based on [32]. We calculate the number of transmission rounds needed to transmit a chunk with size S_n based on the updated $W_{s_n}^{\text{cwnd}}$ and $W_{s_n}^{\text{ssthresh}}$. This calculation assumes that in each round, the total data transmitted is the minimum of the Bandwidth Delay Product (BDP) of the network, or the congestion window, whichever is lower. We model evolution of the congestion window within rounds using typical TCP slow start behavior, and using a simple additive scheme for congestion avoidance. Further, loss events

¹ It is in fact not necessary to observe $B_{s_{1:N}}$, as discussed in the Appendix.

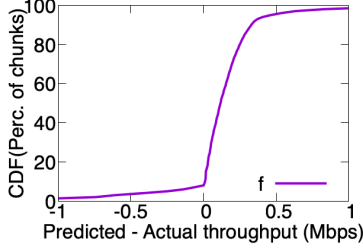


Figure 5: Relative error of f shows acceptable uncertainty.

are not modeled. The number of transmission rounds, the minimum RTT in W_{s_n} , and the chunk size S_n , are all used together to estimate the observed throughput of the video chunk. We emphasize that more detailed models that capture intricate details of specific TCP versions can be easily incorporated in Veritas in the future, but the above model, while simple, helps to illustrate the feasibility and potential of Veritas’s overall approach in tackling causal inference.

We test the performance of f in an emulation environment with a server transmitting payloads of different sizes [2KB to 4 MB] to a client, with random intervals of wait time [0.12s to 8s] between transmission of successive payloads. f derives W_{s_n} using the socket stats utility in Linux [4]. The GTBW between client and server is varied from 0.5 to 10 Mbps, and the end to end delay is varied from 5 to 40 ms using mahimahi [31] across experiments. The GTBW and delay is kept constant for a particular experiment. Figure 5 shows a CDF of the relative error between the actual throughput observed by a payload and the throughput estimated by f across all GTBW and delays. In most cases, the predicted throughput is within a range of 1 Mbps of the observed throughput by the payload.

If f were a perfect estimator, we may have modeled emission probabilities as $P(Y_n | W_{s_n}, S_n, C_{s_n} = c) = 1$ if $Y_n = f(c, W_{s_n}, S_n)$, and $P(Y_n | W_{s_n}, S_n, C_{s_n} = c) = 0$ otherwise. To take the uncertainty of f (Figure 5) into consideration, we include a white-noise Gaussian-distributed error with variance σ^2 (a hyperparameter):

$$P(Y_n | W_{s_n}, S_n, C_{s_n} = c) = \text{Normal}(f(c, W_{s_n}, S_n), \sigma^2). \quad (3)$$

Note that the emission in Equation (3) does not account for $C_{s_n+1}, \dots, C_{e_n}$. In practice, this simplification does not have a significant impact in our ability to sample $C_{1:T}$ as our evaluation shows. Also note that Y_n in the DAG of Figure 3 does not depend on $B_{s_n}, B_{s_{n-1}}, \dots$ given W_{s_n}, S_n , and C_{s_n} (and s_n), thus there is no need to use $B_{s_n}, B_{s_{n-1}}, \dots$ in estimator f .

Evolution of the embedded GTBW. We next discuss how we deal with the fact that there may be no observations attached to a particular hidden state C_t , while there may be more than one observation for a different hidden $C_{t'}$, $t, t' \in \{1, \dots, T\}$. We handle this through embedded transitions in $C_{s_{1:N}}$ in a procedure similar to Neal et al. [30]. That is, for $t \in \{1, \dots, T\}$, instead of modeling $P(C_t | C_{t-1})$, we model the transitions $P(C_{s_n} | C_{s_{n-1}})$, where $1 < n \leq N$. For chunks

$n-1$ and n , we will define $P(C_{s_n} = j\epsilon | C_{s_{n-1}} = i\epsilon) = (A^{\Delta_n})_{i,j}$, where $\Delta_n = s_n - s_{n-1}$ and A is as defined in Equation (2).

Sampling $C_{1:T}$. We are now ready to sample from Equation (1) with our Veritas EHMM. For ease of notation, we define $I_{1:N} = (I_1, \dots, I_N)$, where I_n is the discretized capacity index of chunk n , that is, $C_{s_n} = I_n \epsilon$. Then, the maximum likelihood capacity assignment for all chunks will be

$$I_{1:N}^* = \arg \max_{I_{1:N}} \log P(I_{1:N} | Y_{1:N}, W_{s_{1:N}}, S_{1:N}), \quad (4)$$

where

$$P(I_{1:N} | Y_{1:N}, W_{s_{1:N}}, S_{1:N}) = P(C_{s_1} = I_1 \epsilon) \times P(Y_1 | W_{s_1}, S_1, C_{s_1} = I_1 \epsilon) \prod_{n=2}^N A_{I_{n-1}, I_n}^{\Delta_n} P(Y_n | W_{s_n}, S_n, C_{s_n} = I_n \epsilon) \quad (5)$$

and $P(Y_n | W_{s_n}, S_n, C_{s_n} = I_n \epsilon)$ as defined in Equation (3).

To get Equation (4), we use the Viterbi algorithm which searches —via dynamic programming— for the values of $C_{1:T}$ that give the highest likelihood in Equation (5). The vanilla Viterbi algorithm [45] assumes a constant transition matrix, which we replace by A^{Δ_n} in Veritas. More details of the Veritas Viterbi variant is provided in Algorithm 3 in the Appendix.

We will then use Viterbi output (maximum likelihood estimate) to sample hidden states according to the posterior in Equation (1), similar to [14, 34, 36]. For the sampling, we will additionally require the probability $P(C_{s_n} = i\epsilon, C_{s_{n+1}} = j\epsilon | Y_{1:N}, W_{s_{1:N}}, S_{1:N})$ which can be obtained from our variant of the Baum-Welch forward-backward algorithm (see Algorithm 2 in the Appendix). We denote this pair distribution

$$\Gamma_{i,j,n} = P(C_{s_n} = i\epsilon, C_{s_{n+1}} = j\epsilon | Y_{1:N}, W_{s_{1:N}}, S_{1:N}). \quad (6)$$

The sampling algorithm for $C_{s_{1:N}}$ is defined as Algorithm 1. The intermediate values C_t where $t \in \bigcup_{n=2}^N \{s_{n-1} + 1, \dots, s_n - 1\}$ are interpolated from sampled $C_{s_{1:N}}$.

Input: State space C , Length T , Viterbi output $I_{1:N}^*$,

Transition A , Pair distribution Γ

Output: A sampled capacity trace C

$C_{s_N} = I_{s_N}^* \epsilon$

for $n = N - 1$ **to** 1 **do**

$\xi_{n,i} = \Gamma_{i, C_{s_{n+1}}, n+1}, i\epsilon \in C$

$Z_n = \sum_{i \in C} \xi_{n,i}$

$\pi_{n,i} = \xi_{n,i} / Z_n, i\epsilon \in C$

$C_{s_n} \sim \text{Multinomial}(\pi_{n,:})$

end

Algorithm 1: Capacity Sampler. It obtains the last state N as the last state of Viterbi output, then forward samples each state $1 \leq n < N$ based on sampled state $n+1$ and scores defined by Equation (6).

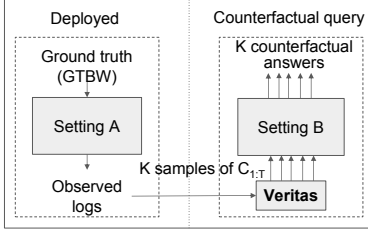


Figure 6: Using Veritas for counterfactual queries.

3.3 How Veritas answers causal queries

Figure 6 shows how Veritas may be used to answer counterfactual and interventional queries. The system deployed in the wild (Setting A) produces logs which for each chunk includes (i) size; (ii) start time of download; (iii) end time of download; and (iv) TCP state including cwnd, ssthresh, and rto [5]. Veritas performs the abduction step, which allows for the sampling K likely GTBW sequences $C_{1:T}$ through Equation (1). The video session is emulated in a new Setting B corresponding to the counterfactual query (e.g., Setting B may correspond to a different algorithm, or buffer size) by replaying each of these sample traces $C_{1:T}$. Veritas then provides K outcomes for the counterfactual query rather than just a single one, capturing the uncertainty inherent in the abduction step given the observed data. While the above description pertains to counterfactual queries, Veritas can also be used for interventional queries as we describe in §4.4.

4 Evaluation

In this section, we evaluate Veritas with respect to how effectively it can respond to causal queries (*what-if* questions) when given traces collected from a video streaming system. We start by evaluating Veritas’s ability to tackle counterfactual queries (§4.1) and then evaluate its effectiveness in handling interventional queries (§4.4).

4.1 Evaluation with counterfactuals

Given traces collected from a video streaming system with a particular set of design decisions, we evaluate the effectiveness of Veritas when answering *what-if* questions related to the performance of the system on *the same set of traces* if one could go back in the past and use a new set of decisions. The decisions that we consider include (i) changing the set of video qualities that the streaming algorithm may choose from; (ii) changing the buffer size available to the video player; and (iii) changing the underlying ABR algorithm itself.

Schemes compared. We compare Veritas’s ability to handle counterfactuals with two approaches:

- **Ground Truth (GTBW):** This refers to the ground truth bandwidth, defined in §3.1. When answering *what-if* questions, results using this technique serve as the ideal benchmark, that Veritas and other approaches must seek to achieve.
- **Baseline:** This scheme directly uses the observed throughput of each chunk, and assumes this throughput value holds

from the start time of the chunk download to the end time of download. During off periods when no estimate is available, linear interpolation of the throughput observed by the previous and next chunks is used. The scheme is commonly used in most video streaming evaluations today. It is expected to be a more accurate representation when the observed throughput is close to GTBW, but underestimates otherwise, and may be inaccurate during off-periods.

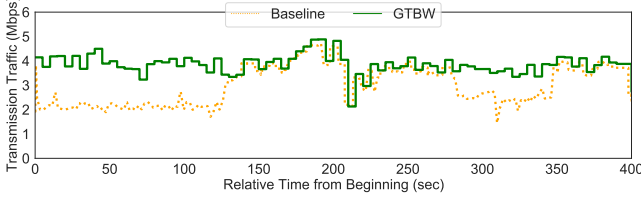
Evaluation setup. When evaluating counterfactual questions, we use the evaluation setup similar to Figure 6. First, we run a video streaming session in Setting A emulating a ground truth network bandwidth (GTBW) trace, which results in a set of logs (as discussed in §3.3). Next, we run the video streaming session in Setting B emulating traces approximating GTBW inferred by Veritas and Baseline, as well as the original GTBW trace. For Veritas, we sample multiple traces (5 by default), and summarize a range of outcomes. We report the performance predicted in Setting B with each of the approaches.

Evaluation metrics. We compare results predicted by each of Veritas, Baseline, and GTBW with respect to the actual *what-if* scenario. Our counterfactual questions pertain to impact of change of setting on the quality of a video session. Hence, we use standard metrics such as video quality (measured by SSIM) and rebuffering ratios.

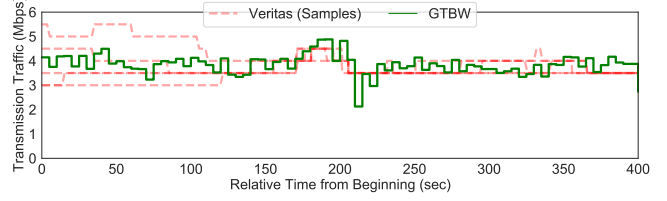
Setup details. We use the evaluation setup provided by Fugu [47] to run our emulation experiments with different ABR algorithms. We emulate FCC throughput traces [1] using Mahimahi [31] to play a 10 minute pre-recorded video clip with bitrate ranging from 0.1 Mbps to 4 Mbps. We use the SSIM index [46] as a measure of video quality. The average SSIM index of lowest quality and highest quality are 0.908 and 0.986 respectively. The clients are launched inside a mahimahi shell with a 80 ms end to end delay and downlink GTBW limited by FCC traces. The GTBW of FCC traces varies from 3 Mbps to 8 Mbps. In our evaluation, we use MPC [48] as default ABR algorithm with a buffer size of 5 seconds. Veritas uses the EHMM described in §3.2 with GTBW transition interval size $\delta=5s$ and minimum GTBW discrepancy $\epsilon=0.5$ Mbps, variance $\sigma=0.5$, a tridiagonal transition matrix A and a uniform initial distribution u through all capacity states. The tridiagonal transition matrix prioritizes GTBW states to be stable, but it allows variation over time. Veritas uses the throughput estimator described in §3.2

4.2 Inference with Veritas: Example

We start by illustrating Veritas’s ability to more accurately infer the GTBW time series compared to Baseline with an example. Figure 7(a) illustrates the GTBW seen during the session for an example trace, as well as the performance observed by Baseline. There are significant periods (e.g. upto 120 seconds, and between 270 and 350 seconds) where Baseline is conservative in its estimation of GTBW. This is because in these periods the deployed ABR algorithm selects smaller



(a) GTBW and Baseline.



(b) GTBW and Veritas samples.

Figure 7: Comparing Baseline, GTBW and Veritas samples for an example trace.

chunk sizes (either lower qualities, or lower-sized chunks of higher quality given variable bit rate video). Consequently, observed throughput in these periods is significantly lower than GTBW.

Figure 7(b) illustrates the time series reconstructed by Veritas for the same GTBW trace. Veritas does not provide one single trace, but allows sampling of multiple candidate traces, with more probable traces having a higher likelihood of being sampled. The figure shows five sample traces from Veritas. We make several observations. First, all these samples are closer to GTBW than Baseline. Second, in regions where Baseline is close to GTBW (e.g., between 120 and 270 seconds), all samples from Veritas are also close to GTBW. This is because in these regions, the chunk sizes selected by the deployed algorithm exceed the bandwidth delay product (BDP) of the network. Here, the observed throughput is closer to GTBW, and Veritas is relatively more certain. Third, in regions where Baseline is conservative, all Veritas samples are significantly less conservative. However, in some of these regions (e.g., 0 to 120 seconds), Veritas exhibits more uncertainty. This occurs because if smaller chunk sizes are chosen by the deployed algorithm, a range of different GTBW values may have resulted in the same throughput observations. This is intrinsic, reflecting the uncertainty inherent in the available data. Note that Veritas’s use of HMMs allows it to pick more probable samples based on transition probabilities (i.e., since it infers GTBW in some regions with higher certainty, the transition probabilities constrain the range of GTBW possibilities in the less certain regions).

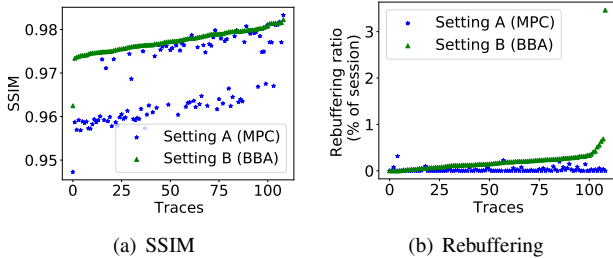


Figure 8: True impact of changing ABR algorithm from MPC to BBA.

4.3 Results: Veritas with counterfactuals

We next evaluate Veritas’s ability to answer three example counterfactual questions.

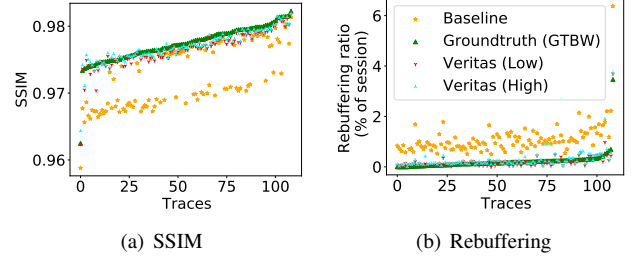


Figure 9: Predicted performance if ABR was changed from MPC to BBA.

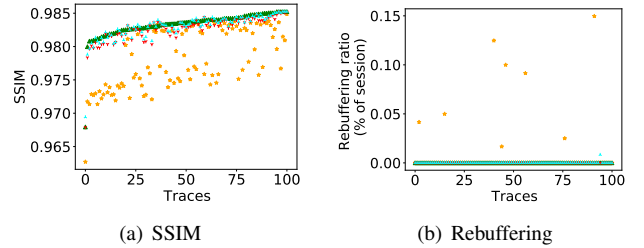


Figure 10: Predicted performance if buffer size was increased to 30s.

Change of ABR algorithm. Consider that the video streaming application has been deployed with a given ABR. We ask the counterfactual *what would have happened if an alternate ABR algorithm were instead used*. We study this question in the context of moving from the MPC algorithm [48] to the BBA algorithm [18]. Figures 8(a) and 8(b) show the SSIM and rebuffering ratio achieved by MPC and BBA when using the same set of GTBW traces. In each graph, each point on the X-Axis corresponds to a GTBW trace, and each graph plots the SSIM (or rebuffering ratio) for that trace with the two algorithms. Notice that BBA is more aggressive with larger SSIM values and higher rebuffering.

We next evaluate the ability of Baseline and Veritas to predict the impact on video performance if (i) logs from a deployment of the MPC algorithm were provided; and (ii) the BBA algorithm were used instead. For each video session, we infer five sample GTBW time series using Veritas, and emulate each video session under each of the five Veritas samples. Each sample provides a prediction of SSIM and rebuffering with Veritas. We consider the second lowest and second largest prediction for each metric across the samples, which we refer to as Veritas (Low) and Veritas (High) respec-

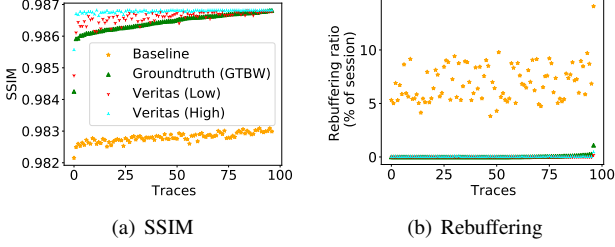


Figure 11: Predicted performance if higher video qualities were used.

tively. This provides a range of predictions with Veritas for each trace.

Figures 9(a) and 9(b) present the SSIM and rebuffering ratio predicted by Baseline and Veritas. The true impact of the change (GTBW) is also shown for comparison. The graph shows that Baseline predicts a noticeably lower SSIM than GTBW², and a significantly higher rebuffering ratio. This is because Baseline underestimates GTBW as we have seen. In contrast, the range of estimates from Veritas is close to GTBW across the traces and fairly tight indicating Veritas is confident in assessing the impact of this change.

In the Appendix, we have also evaluated the impact of changing from MPC to the BOLA algorithm, which shows similar results: Veritas does a good job of predicting the impact of the change, but Baseline does not.

Change of buffer size. Consider that the video streaming application has been deployed with an ABR and a buffer size. The designer then asks: *what would have been the performance if a different buffer size had been used?* Intuitively, increasing the buffer size should improve video quality and lower rebuffering, but lower the liveness for the application. We deploy the MPC algorithm with a buffer size of 5 seconds (Setting A), and using the logs so obtained, evaluate the impact predicted by different schemes if the buffer size were increased to 30 seconds (Setting B). Figures 10(a) and 10(b) show the results. Veritas accurately predicts SSIM and rebuffering ratio (close to GTBW), with the range of estimates for each trace being relatively tight. Baseline underestimates SSIM for most traces, and slightly over-estimates rebuffering ratios for some traces.

Change of qualities. Consider that the video streaming application has been deployed with a given set of video qualities. We next consider the counterfactual: *what would be the impact if a higher set of qualities were used instead?* Figure 11 shows that Veritas achieves SSIM and rebuffering close to GTBW. However, Baseline underestimates SSIM and significantly overestimates rebuffering (the estimates of rebuffering ratio with Baseline are in the 5-10% range across traces, while the estimates are close to 0 with GTBW and Veritas for most traces). Note that for this case study, Veritas tends

²Average bit rate for the median trace reduces from the true value of 3.5 Mbps to 3.1 Mbps for baseline. See Appendix which presents the impact on average bit rate for all counterfactual queries.

to slightly over-estimate SSIM relative to GTBW. This is because in most traces in the deployment, the downloaded chunk sizes were under the bandwidth delay product, leading to a wide range of possible GTBW time series consistent with the observed throughput values. Such variance is inherent to the information in the data. Veritas can provide a range of outcomes in general, and obtaining more samples could potentially lead to lower estimates. Overall, Veritas is effective in answering the counterfactuals and far more accurate than Baseline.

4.4 Evaluations on interventionals

So far, we have evaluated Veritas on counterfactual queries that involve evaluation on a trace if one could go back to the past and change the setting. We next evaluate Veritas’s potential for interventional queries, which relate to the future (§2), focusing on the ability to predict chunk download times in a bias-free fashion. We compare two schemes:

- **FuguNN:** This refers to a neural network proposed in [47] which predicts the download time of chunks based on the sizes and download times of prior chunks. While the approach is effective at predicting chunk download times for sizes selected by the deployed ABR, it suffers from a bias when predicting download times for alternate chunk sizes different than what the deployed ABR may have selected as shown in §2.1.
- **Veritas:** Using only the chunks downloaded upto a particular point in the session, we use Veritas to infer GTBW time series for the past. We consider a single sample from Veritas corresponding to the most likely one. We then use the transition matrix to get the expected value of GTBW for the next chunk.

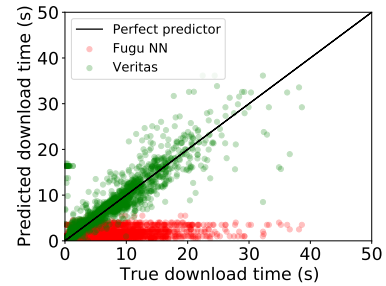


Figure 12: Comparing FuguNN and HMM for download time prediction in an interventional context.

We train FuguNN using traces obtained by running the MPC algorithm on 100 FCC traces sampled uniformly from all traces with average GTBW values ranging from 0.5 to 10 Mbps. We then create a separate set of 30 traces drawn from the same range of GTBW, but where bit rates are selected randomly rather than use an ABR algorithm to serve as a test set. The purpose is to evaluate FuguNN and Veritas on their ability to predict chunk download times for arbitrary chunk sequences, not specific to what one may encounter in the deployed algorithm. Each test trace gives us ground truth information for the size and download time for several chunk

sequences. We then run FuguNN and Veritas offline for every chunk sequence of each trace, and obtain the download time predicted by each of these methods. The results are shown in Figure 12. FuguNN underestimates the download time due to its associational model and is unable to estimate correctly for interventional queries that involve chunk sequences different than what one might expect with the deployed ABR. Veritas however can effectively handle such interventional queries. Note that as discussed in §2.2, this is important when using FuguNN as a predictor in a live session since at each time step, it is used to predict the download times for *all possible chunk sizes* (not just the size the deployed algorithm would have selected).

5 Related Work

- **Biases with video streaming.** A very recent parallel work [7] and a preliminary workshop paper [39] are motivated by similar goals as this paper. However, [39] is restricted to a square wave bandwidth process, does not model the dependence of observed throughput on chunk size, or handle the uncertainty in inference. Finally, the use of matching in [39] requires bitrates to be occasionally chosen randomly. [7] has an RCT requirement in the training phase where each of N sessions is assigned to one of K ABR policies completely at random, and proposes counterfactual estimation as a matrix completion task. As discussed in Section 2.3, it is unclear how such approaches can evaluate actions that were outside the scope of the initial RCT experiment (e.g., what if the ABR now allowed 8K videos, or could use a different buffer size?). Moreover, deploying RCT ABR algorithms to collect traces can impact the performance of real-world users. In contrast, our work does not require RCT traces and can answer any *what-if* query without constraints.

Another work [10] has observed that smaller chunk sizes may see poorer throughput than larger ones owing to TCP slow start effects. To handle this, [10] compares the total reward seen by algorithm B on a trace collected from an algorithm A by only considering those chunks where the new algorithm picks the same bitrate as the old algorithm. The approach does not tackle *what-if* questions, assumes a constant bandwidth process, and does not model the causal dependence of chunk size selection by the ABR algorithm on bandwidth. We tackle the harder problem of inferring a latent and variable bandwidth process from observed throughput, deal with the uncertainty in such inference, and address a wide range of causal *what-if* queries.

- **Inferring causal dependencies and *what-if* analysis.** Several works [21, 25, 42] infer causal dependencies using correlations but do not consider latent confounders. Some work [16, 21, 22, 43] deals with observed confounders – e.g., Krishnan et al. [22] explored whether video stream quality (e.g., rebuffering ratios) causally impacts user engagement metrics while accounting for observed confounders such as user connection type (DSL vs. mobile) and location. These

works only infer if a correlation is an indication of a causal relationship but do not answer *what-if* questions, and do not deal with latent confounders. Other works [20, 37, 42] consider *what if* analyses for various applications, but do not address confounding variables.

Recent work [23] considers causal questions while considering implicit feedback in the context of cloud systems – e.g., when a system waits X minutes for an event to occur, there is implicit feedback in terms of what would have happened if a smaller wait time were used. This approach relies on randomized experiments (from RL exploration) and, thus, does not need to explicitly consider all possible confounders. In contrast, we are interested in scenarios where randomized experiments are limited or not available.

6 Conclusion

In this paper, we have made three contributions. First, we have shown causal reasoning is complex with ABR video, since the quality of selected video chunks is causally dependent on GTBW, which acts as a sequence of latent and confounding variables. Second, we present Veritas, a novel framework that tackles causal reasoning for video streaming without resorting to randomized trials. Veritas uses an embedded Hidden Markov Model that relates the latent GTBW time series to throughput observed by the application. A key insight behind Veritas is exploiting information about the TCP state at the start of each chunk download to simplify the causal inference. Third, we show the effectiveness of Veritas in answering a wide range of counterfactual and interventional queries through emulation testbed experiments. For example, when predicting the impact of using higher video qualities, Veritas predicts negligible rebuffering ratios, matching ground truth. However, Baseline (which does not adjust for causal effects) predicts much higher median rebuffering ratios (6.7%). With interventional queries related to chunk download times, Veritas predicts download times close to true values, while Fugu’s associational approach can underestimate chunk download times by 5.8 seconds for 10% of the chunks, and underestimate download times by as much as 35 seconds in the worst case.

References

- [1] Federal communications commission. 2016. raw data - measuring broadband america. (2016). <https://www.fcc.gov/reports-research/reports/measuring-broadband-america/raw-data-measuring-broadband-america-2016>.
- [2] Implementing BOLA-BASIC on puffer. <https://puffer.stanford.edu/bola/#footnote-1>.
- [3] Netflix and YouTube agree to reduce bitrate during Coronavirus crisis. <https://www.broadbandtvnews.com/2020/03/19/netflix-agrees-to-reduce-bitrate-during-coronavirus-crisis/>.

- [4] ss - Linux manual page. <https://man7.org/linux/man-pages/man8/ss.8.html>.
- [5] tcp - Linux manual page. <https://man7.org/linux/man-pages/man7/tcp.7.html>.
- [6] Zahaib Akhtar, Yun Seong Nam, Ramesh Govindan, Sanjay Rao, Jessica Chen, Ethan Katz-Bassett, Bruno Ribeiro, Jibin Zhan, and Hui Zhang. Oboe: auto-tuning video ABR algorithms to network conditions. In *Proceedings of the 2018 Conference of the ACM Special Interest Group on Data Communication - SIGCOMM '18*, pages 44–58, Budapest, Hungary, 2018. ACM Press.
- [7] Abdullah Alomar, Pouya Hamadani, Arash Nasr-Esfahany, Anish Agarwal, Mohammad Alizadeh, and Devavrat Shah. Causalsim: Toward a causal data-driven simulator for network protocols. *arXiv preprint arXiv:2201.01811*, 2022.
- [8] Joshua D Angrist, Guido W Imbens, and Donald B Rubin. Identification of causal effects using instrumental variables. *Journal of the American statistical Association*, 91(434):444–455, 1996.
- [9] Elias Bareinboim, Andrew Forney, and Judea Pearl. Bandits with unobserved confounders: A causal approach. *Advances in Neural Information Processing Systems*, 28:1342–1350, 2015.
- [10] Mihovil Bartulovic, Junchen Jiang, Sivaraman Balakrishnan, Vyas Sekar, and Bruno Sinopoli. Biases in Data-Driven Networking, and What to Do About Them. In *Proceedings of the 16th ACM Workshop on Hot Topics in Networks - HotNets- XVI*, pages 192–198, Palo Alto, CA, USA, 2017. ACM Press.
- [11] Eli Bingham, Jonathan P Chen, Martin Jankowiak, Fritz Obermeyer, Neeraj Pradhan, Theofanis Karaletsos, Rohit Singh, Paul Szerlip, Paul Horsfall, and Noah D Goodman. Pyro: Deep Universal Probabilistic Programming. *Journal of Machine Learning Research*, 20(28):1–6, 2019.
- [12] Ethan Blanton, Dr. Vern Paxson, and Mark Allman. TCP Congestion Control. RFC 5681, September 2009.
- [13] Bob Carpenter, Andrew Gelman, Matthew D. Hoffman, Daniel Lee, Ben Goodrich, Michael Betancourt, Marcus Brubaker, Jiqiang Guo, Peter Li, and Allen Riddell. Stan: A Probabilistic Programming Language. *Journal of Statistical Software*, 76(i01), 2017.
- [14] Siddhartha Chib. Calculating posterior distributions and modal estimates in markov mixture models. *Journal of Econometrics*, 75(1):79–97, 1996.
- [15] Angus Deaton and Nancy Cartwright. Understanding and misunderstanding randomized controlled trials. *Social Science & Medicine*, 210:2–21, August 2018.
- [16] Hadrien Hours, Ernst Biersack, and Patrick Loiseau. A Causal Approach to the Study of TCP Performance. *ACM Transactions on Intelligent Systems and Technology*, 7(2):25:1–25:25, December 2015.
- [17] Te-Yuan Huang, Ramesh Johari, Nick McKeown, Matthew Trunnell, and Mark Watson. A buffer-based approach to rate adaptation: Evidence from a large video streaming service. In *Proceedings of the 2014 ACM Conference on SIGCOMM*, SIGCOMM '14, pages 187–198, New York, NY, USA, 2014. ACM.
- [18] Te-Yuan Huang, Ramesh Johari, Nick McKeown, Matthew Trunnell, and Mark Watson. A buffer-based approach to rate adaptation: Evidence from a large video streaming service. In *Proceedings of the 2014 ACM Conference on SIGCOMM*, SIGCOMM '14, 2014.
- [19] Junchen Jiang, Vyas Sekar, and Hui Zhang. Improving fairness, efficiency, and stability in http-based adaptive video streaming with festive. In *Proceedings of the 8th International Conference on Emerging Networking Experiments and Technologies*, CoNEXT '12, pages 97–108, New York, NY, USA, 2012. ACM.
- [20] Yurong Jiang, Lenin Ravindranath Sivalingam, Suman Nath, and Ramesh Govindan. WebPerf: Evaluating What-If Scenarios for Cloud-hosted Web Applications. In *Proceedings of the Conference of the ACM Special Interest Group on Data Communication - SIGCOMM '16*, pages 258–271, Florianopolis, Brazil, 2016. ACM Press.
- [21] Satoru Kobayashi, Kazuki Otomo, Kensuke Fukuda, and Hiroshi Esaki. Mining Causality of Network Events in Log Data. *IEEE Transactions on Network and Service Management*, 15(1):53–67, March 2018.
- [22] S. Shunmuga Krishnan and Ramesh K. Sitaraman. Video stream quality impacts viewer behavior: inferring causality using quasi-experimental designs. In *Proceedings of the 2012 Internet Measurement Conference*, IMC '12, pages 211–224, Boston, Massachusetts, USA, November 2012. Association for Computing Machinery.
- [23] Mathias Lécuyer, Sang Hoon Kim, Mihir Nanavati, Junchen Jiang, Siddhartha Sen, Aleksandrs Slivkins, and Amit Sharma. *Sayer: Using Implicit Feedback to Optimize System Policies*. ACM Symposium on Cloud Computing (SOCC), New York, NY, USA, 2021.
- [24] Xi Liu, Florin Dobrian, Henry Milner, Junchen Jiang, Vyas Sekar, Ion Stoica, and Hui Zhang. A case for a

- coordinated internet video control plane. *ACM SIGCOMM Computer Communication Review*, 42(4):359–370, 2012.
- [25] Ajay Anil Mahimkar, Zihui Ge, Aman Shaikh, Jia Wang, Jennifer Yates, Yin Zhang, and Qi Zhao. Towards automated performance diagnosis in a large IPTV network. *ACM SIGCOMM Computer Communication Review*, 39(4):231–242, 2009. Publisher: ACM New York, NY, USA.
- [26] Hongzi Mao, Ravi Netravali, and Mohammad Alizadeh. Neural adaptive video streaming with pensieve. In *Proceedings of the Conference of the ACM Special Interest Group on Data Communication*, pages 197–210. ACM, 2017.
- [27] Tom Mitchell and Machine Learning McGraw-Hill. Edition, 1997.
- [28] Yun Seong Nam, Jianfei Gao, Chandan Bothra, Ehab Ghabashneh, Sanjay Rao, Bruno Ribeiro, Jibin Zhan, and Hui Zhang. Xatu: Richer neural network based prediction for video streaming. *ACM SIGMETRICS*, 2022.
- [29] Siddharth Narayanaswamy, Brooks Paige, Jan-Willem van de Meent, Alban Desmaison, Noah D. Goodman, Pushmeet Kohli, Frank D. Wood, and Philip H. S. Torr. Learning disentangled representations with semi-supervised deep generative models. In *NIPS*, pages 5927–5937, 2017.
- [30] Radford Neal, Matthew Beal, and Sam Roweis. Inferring state sequences for non-linear systems with embedded hidden markov models. *Advances in neural information processing systems*, 16, 2003.
- [31] Ravi Netravali, Anirudh Sivaraman, Keith Winstein, Somak Das, Ameesh Goyal, and Hari Balakrishnan. Mahimahi: A lightweight toolkit for reproducible web measurement. In *Proceedings of the 2014 ACM Conference on SIGCOMM*, SIGCOMM ’14, page 129–130, New York, NY, USA, 2014. Association for Computing Machinery.
- [32] Jitendra Padhye, Sally Floyd, and Mark J. Handley. TCP Congestion Window Validation. RFC 2861, June 2000.
- [33] Judea Pearl. *Causality*. Cambridge university press, 2009.
- [34] Christian P Robert and DM Titterton. Reparameterization strategies for hidden markov models and bayesian approaches to maximum likelihood estimation. *Statistics and Computing*, 8(2):145–158, 1998.
- [35] Kenneth J. Rothman and Sander Greenland. Causation and causal inference in epidemiology. *American Journal of Public Health*, 95 Suppl 1:S144–150, 2005.
- [36] Steven L Scott. Bayesian analysis of a two-state markov modulated poisson process. *Journal of Computational and Graphical Statistics*, 8(3):662–670, 1999.
- [37] Rahul Singh, Prashant Shenoy, Maitreya Natu, Vaishali Sadaphal, and Harrick Vin. Analytical modeling for what-if analysis in complex cloud computing applications. *ACM SIGMETRICS Performance Evaluation Review*, 40(4):53–62, April 2013.
- [38] Kevin Spiteri, Rahul Ugaonkar, and Ramesh K Sitaraman. Bola: Near-optimal bitrate adaptation for online videos. In *IEEE INFOCOM 2016-The 35th Annual IEEE International Conference on Computer Communications*, pages 1–9. IEEE, 2016.
- [39] P. C. Sruthi, Sanjay Rao, and Bruno Ribeiro. Pitfalls of data-driven networking: A case study of latent causal confounders in video streaming. In *Proceedings of the Workshop on Network Meets AI & ML, NetAI ’20*, page 42–47, New York, NY, USA, 2020. Association for Computing Machinery.
- [40] Yi Sun, Xiaoqi Yin, Junchen Jiang, Vyas Sekar, Fuyuan Lin, Nanshu Wang, Tao Liu, and Bruno Sinopoli. Cs2p: Improving video bitrate selection and adaptation with data-driven throughput prediction. In *Proceedings of the 2016 ACM SIGCOMM Conference*, pages 272–285, 2016.
- [41] Charles Sutton and Andrew McCallum. An Introduction to Conditional Random Fields for Relational Learning. *Graph. Models*, 7:93, 2002.
- [42] Mukarram Tariq, Amgad Zeitoun, Vytas Valancius, Nick Feamster, and Mostafa Ammar. Answering what-if deployment and configuration questions with wise. In *Proceedings of the ACM SIGCOMM 2008 Conference on Data communication*, pages 99–110, 2008.
- [43] Mukarram Bin Tariq, Murtaza Motiwala, Nick Feamster, and Mostafa Ammar. Detecting network neutrality violations with causal inference. In *Proceedings of the 5th International Conference on Emerging Networking Experiments and Technologies*, pages 289–300, 2009.
- [44] Guibin Tian and Yong Liu. Towards agile and smooth video adaptation in dynamic http streaming. In *Proceedings of the 8th International Conference on Emerging Networking Experiments and Technologies, CoNEXT ’12*, 2012.
- [45] Andrew J Viterbi. A personal history of the viterbi algorithm. *IEEE Signal Processing Magazine*, 23(4):120–142, 2006.

- [46] Zhou Wang, A.C. Bovik, H.R. Sheikh, and E.P. Simoncelli. Image quality assessment: from error visibility to structural similarity. *IEEE Transactions on Image Processing*, 13(4):600–612, 2004.
- [47] Francis Y. Yan, Hudson Ayers, Chenzhi Zhu, Sadjad Fouladi, Jañes Hong, Keyi Zhang, Philip Levis, and Keith Winstein. Learning in situ: a randomized experiment in video streaming. In *17th USENIX Symposium on Networked Systems Design and Implementation (NSDI 20)*, pages 495–511, 2020.
- [48] Xiaoqi Yin, Abhishek Jindal, Vyas Sekar, and Bruno Sinopoli. A control-theoretic approach for dynamic adaptive video streaming over http. In *Proceedings of the 2015 ACM Conference on Special Interest Group on Data Communication, SIGCOMM ’15*, London, United Kingdom, 2015.

A Appendix

A.1 Further Results

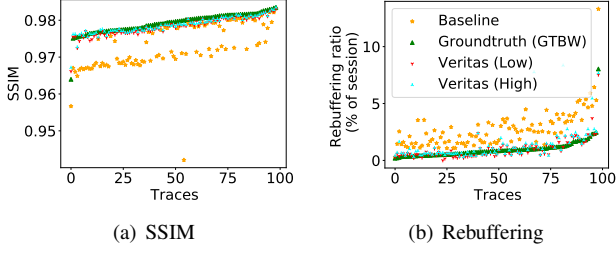
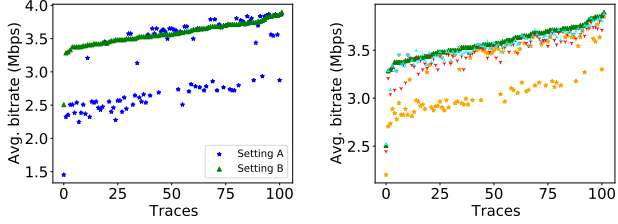
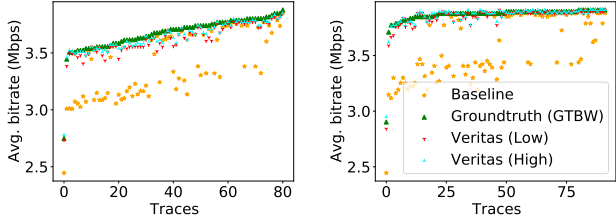


Figure 13: Change of ABR from MPC to Bola.

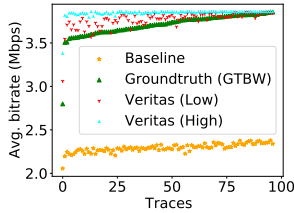
Figure 13(b) and Figure 13(a) show the SSIM and rebuffering ratio predicted by Veritas and Baseline when we change the algorithm from MPC and Bola [38]. We use the Bola Basic V1 algorithm implemented in the Puffer setup for this analysis [2]. The results are similar to that of changing the ABR from MPC to BBA. Baseline underestimates the GTBW which leads to lower SSIM and higher rebuffering. Veritas does a good job of predicting the impact of the change, but Baseline does not.



(a) Avg. bitrate in Setting A and B (MPC and BBA). (b) Avg. bitrate for change from MPC to BBA.



(c) Avg. bitrate for change from MPC to Bola. (d) Avg. bitrate for changing buffer size.



(e) Avg. bitrate for changing qualities.

Figure 14: Avg. bitrate for counterfactual queries.

Figure 14 compares the Avg. bitrate for Baseline and Veritas

with GTBW for various counterfactual queries.

A.2 Model and Algorithms

In this part, we will clarify some details of our models and present pseudo code for all algorithms: Viterbi variant, Baum-Welch forward-backward variant and network throughput estimator used in our EHMM.

Why $B_{s_{1:N}}$ need not be observed. In Figure 3's DAG, start time $s_{1:N}$ are not defined as random variables to simplify exposition. If we had defined $s_{1:N}$ as an observed random variable, $s_{1:N}$ could have been used in place of $B_{s_{n-1}}$ to define the sufficient set of observed variables in our d -separation argument. Looking at the dependence between $P(C_{s_n} = j\epsilon | C_{s_{n-1}} = i\epsilon)$ and Δ_n makes it clear that observing $s_{1:N}$ is also necessary for our Markov model. To conclude, then, we do not actually need to log $B_{s_{1:N}}$ since $s_{1:N}$ is necessary and sufficient and readily available in the trace.

Algorithm Pseudo Codes. As introduced in Section 3.2, our Viterbi and Baum-Welch forward-backward variants are nearly the same as their origins, but replace the transition matrix from constant matrix A to A^{Δ_n} where Δ_n is as shown in Section 3.2 and Figure 4, and replace the emission process by our proposal as Equation (3). The pseudo codes of both algorithms are provided in Algorithm 3 and Algorithm 2.

We use a simple model f , which estimates throughput given GTBW, TCP state and size of related download chunk. The pseudo code is provided in Algorithm 4.

Input: State Space \mathcal{C} , Transition times T , Initial distribution u_1 , Transition matrix A , Emission process E (Equation (3)), Throughputs $Y_{1:N}$, TCP states $W_{s_{1:N}}$, Chunk sizes $S_{1:T}$, interval gaps Δ , capacity unit ϵ

Output: Conditional Joint Distribution Γ

```

/* Alias */
 $\xi_{i,j,n}^{\text{back}} = A_{i,j}^{\Delta_n} E(Y_n, W_{s_n}, S_n | j\epsilon), \forall i, j \in \mathcal{C}, \forall 2 \leq n \leq N$ 
 $\xi_{i,j,n}^{\text{fore}} = A_{i,j}^{\Delta_{n+1}} E(Y_{n+1}, W_{s_{n+1}}, S_{n+1} | j\epsilon), \forall i, j \in \mathcal{C}, \forall 1 \leq n \leq N-1$ 
/* Forward */
 $\alpha_{1,i} = u_{1,i} E(Y_1, W_{s_1}, S_1 | i\epsilon), \forall i \in \mathcal{C}$ 
for  $n = 2 \rightarrow N$  do
     $\alpha_{n,i} = \sum_{j \in \mathcal{C}} \alpha_{n-1,j} \xi_{j,i,n}^{\text{back}}, \forall i \in \mathcal{C}$ 
end
/* Backward */
 $\beta_{N,i} = 1, \forall i \in \mathcal{C}$ 
for  $n = N-1 \rightarrow 1$  do
     $\beta_{n,i} = \sum_{j \in \mathcal{C}} \xi_{i,j,n}^{\text{fore}} \beta_{n+1,j}, \forall i \in \mathcal{C}$ 
end
/* Posterior */
for  $n = 1 \rightarrow N-1$  do
    for  $i \in \mathcal{C}$  do
        for  $j \in \mathcal{C}$  do
             $\Gamma_{i,j,n} = \frac{\alpha_{n,i} \xi_{i,j,n}^{\text{fore}} \beta_{n+1,j}}{\sum_{k \in \mathcal{C}} \sum_{l \in \mathcal{C}} \alpha_{n,k} \xi_{k,l,n}^{\text{fore}} \beta_{n+1,l}}$ 
        end
    end
end

```

Algorithm 2: Forward-Backward Algorithm. It first computes forward distribution $\alpha_{n,i} = P(C_{s_n} = i\epsilon | Y_{1:n}, W_{s_{1:n}}, S_{1:n})$; then computes backward distribution $\beta_{n,i} = P(C_{s_n} = i\epsilon | Y_{n+1:N}, W_{s_{n+1:N}}, S_{n+1:N})$; and finally achieve conditional joint distribution $\Gamma_{i,j,n} = P(C_{s_n} = i\epsilon, C_{s_{n+1}} = j\epsilon | Y_{1:N}, W_{s_{1:N}}, S_{1:N})$ by combining α and β for all i, j in GTBW state space from 1 to $N-1$ chunks.

Input: State Space \mathcal{C} , Transition times T , Initial distribution u_1 , Transition matrix A , Emission process E (Equation (3)), Throughputs $Y_{1:N}$, TCP states $W_{s_{1:N}}$, Chunk sizes $S_{1:T}$, interval gaps Δ , capacity unit ϵ

Output: Most Likely State Trace I^*

```

 $\xi_{1,i} = u_{1,i} E(Y_1, W_{s_1}, S_1 | i\epsilon), \forall i \in \mathcal{C}$ 
for  $n = 2 \rightarrow N$  do
     $x_{n,i} = \arg \max_{j \in \mathcal{C}} \xi_{1,j} A_{j,i}^{\Delta_n} E(Y_n, W_{s_n}, S_n | i\epsilon), \forall i \in \mathcal{C}$ 
     $\xi_{n,i} = \xi_{1,x_{n,i}} A_{x_{n,i},i}^{\Delta_n} E(Y_n, W_{s_n}, S_n | i\epsilon), \forall i \in \mathcal{C}$ 
end
 $I_N^* = \arg \max_{i \in \mathcal{C}} \xi_{N,i}$ 
for  $n = N-1 \rightarrow 1$  do
     $I_n^* = x_{n+1, I_{n+1}^*}$ 
end

```

Algorithm 3: Viterbi Algorithm. It can search for the most likely GTBW state trace I^* which can generate given observations $Y_{1:N}, W_{s_{1:N}}, S_{1:N}$, on all chunks through dynamic programming.

Input: C , TCP state W_{S_n} , Chunk size S_n
Output: Y_n

```

/* Calculating ssthresh and cwnd. */
if  $W_{S_n}^{last\_snd} > W_{S_n}^{rto}$  then
    /* Slow start restart. */
     $init\_cwnd \leftarrow 10$ 
    while  $((W_{S_n}^{last\_snd} - W_{S_n}^{rto}) > 0)$  and
         $(W_{S_n}^{cwnd} > init\_cwnd)$  do
         $W_{S_n}^{last\_snd} = W_{S_n}^{last\_snd} - W_{S_n}^{rto}$ 
         $W_{S_n}^{cwnd} \leftarrow W_{S_n}^{cwnd} \ll 2$ 
    end
     $W_{S_n}^{ssthresh} \leftarrow \max(W_{S_n}^{ssthresh}, (W_{S_n}^{cwnd} >> 1) + (W_{S_n}^{cwnd} >> 2))$ 
end
/* Get number of data segments. */
 $data\_segments \leftarrow get\_segments(S_n)$ 
 $bdp\_segments \leftarrow get\_segments(GTBW * W_{S_n}^{min\_rtt})$ 
if  $W_{S_n}^{cwnd} > bdp\_segments$  then
    if  $data\_segments > bdp\_segments$  then
        return  $C$ 
    else
        return  $S_n / W_{S_n}^{min\_rtt}$ 
    end
else
     $rounds \leftarrow 0$ 
     $sent \leftarrow 0$ 
    while  $sent < data\_segments$  do
         $sent \leftarrow sent + \min(W_{S_n}^{cwnd}, bdp\_segments)$ 
        if  $W_{S_n}^{cwnd} < W_{S_n}^{ssthresh}$  then
             $W_{S_n}^{cwnd} \leftarrow 2 * W_{S_n}^{cwnd}$ 
        else
             $W_{S_n}^{cwnd} \leftarrow W_{S_n}^{cwnd} + 1$ 
        end
         $rounds \leftarrow rounds + 1$ 
    end
    return  $\min((S_n / (rounds * W_{S_n}^{min\_rtt})), C)$ 
end

```

Algorithm 4: Network throughput estimator: f